OXFORD

Food Quality and Safety, 2020, 4, 203–212
doi:10.1093/fqsafe/fyaa016
Article
Advance Access publication 28 August 2020

Article

Chemical characterization, release, and bioactivity of *Eucalyptus camaldulensis* polyphenols from freeze-dried sodium alginate and sodium carboxymethyl cellulose matrix

Ozioma Forstinus Nwabor, Sudarshan Singh, Dwi Marlina and Supayang Piyawan Voravuthikunchai

Excellence Research Laboratory on Natural Products, Department of Microbiology, Faculty of Science and Natural Product Research Center of Excellence, Prince of Songkla University, Hat Yai, Songkhla, Thailand

Correspondence to: Supayang Piyawan Voravuthikunchai, Excellence Research Laboratory on Natural Products, Department of Microbiology, Faculty of Science and Natural Product Research Center of Excellence, Prince of Songkla University, Hat Yai, Songkhla 90112, Thailand. E-mail: supayang.v@psu.ac.th

Received 2 February 2020; Revised 3 April 2020; Editorial decision 3 April 2020.

Abstract

Crude ethanolic extract of *Eucalyptus camaldulensis* was encapsulated with sodium alginate–sodium carboxymethyl cellulose (CMC) using freeze-drying techniques. The microcapsules were characterized for particle size, morphology, physicochemical parameters, and micromeritics properties. Antioxidant and antimicrobial activities of the microcapsules were also demonstrated. Results revealed an irregular-shaped microparticles with a mean diameter ranging from 6.7 to 26.6 μm. Zeta potential and polydispersity index ranged from –17.01 to 2.23 mV and 0.34 to 0.49, respectively. Percentage yield ranged between 70.4 and 81.5 per cent whereas encapsulation efficiency ranged between 74.2 ± 0.011 and 82.43 ± 0.77 per cent. Swelling index and solubility varied inversely with extract concentration, with a range of 54.4%–84.0% and 18.8%–22.2%, respectively. Antioxidant activities varied directly with the concentration of the extract. Minimum inhibitory and minimum bactericidal concentrations of the microcapsules against Gram-positive foodborne pathogens ranged from 0.19 to 3.12 and 0.19–12.25 mg/ml, respectively. The Higuchi model indicated a time-dependent, delayed, and regulated release of polyphenols at 37°C. The results suggested that alginate–CMC possessed good encapsulant properties that preserved the bioactive extract, thus might be employed for application of natural products in food systems.

Graphical Abstract

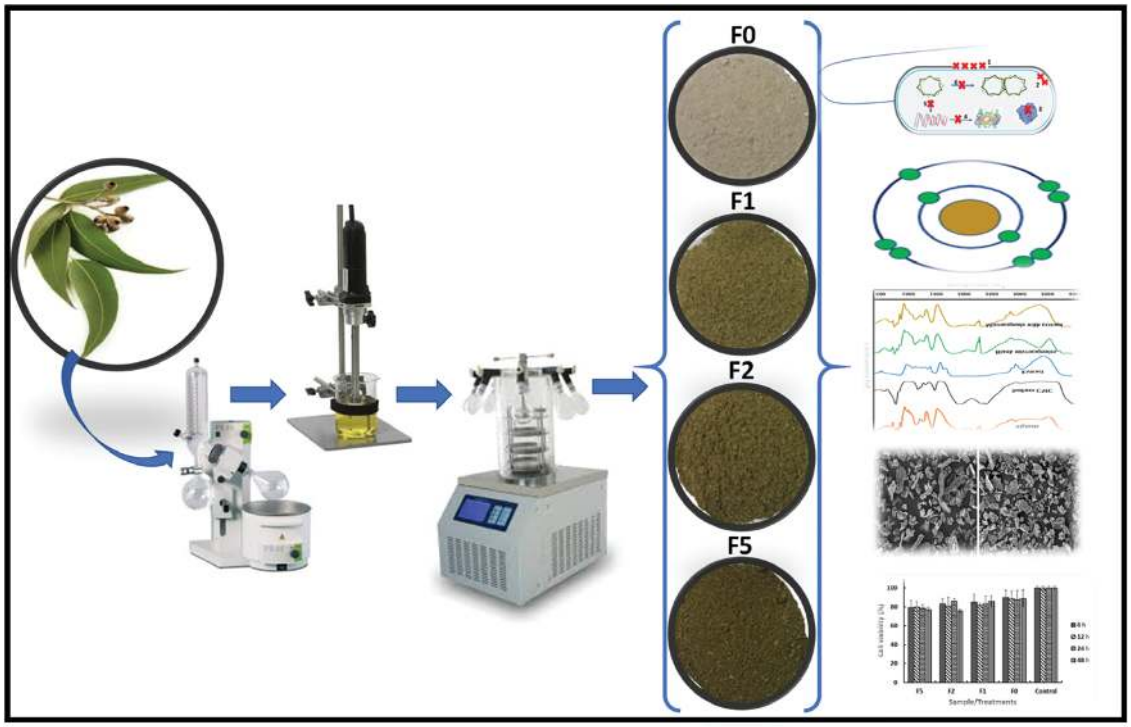

Key words: microencapsulation, freeze-drying, antimicrobial, antioxidant, *Eucalyptus camaldulensis*, regulated release.

Introduction

The growing demand for natural products in food and other consumables and overall distaste for synthetic chemicals have resulted in heightened search for appropriate methods of incorporating inert natural products into processing systems. Plant extracts and phenolic compounds are healthy sources of green components that might replace or limit the use of synthetic chemicals. Numerous plants have demonstrated bioactive properties that can be exploited in the development of useful consumer products. Plant extracts, essential oils, and phenolic phytochemicals have been employed as preservatives (Dhiman and Aggarwal, 2019), flavours, colouring agents (Dikshit and Tallapragada, 2018; Allahdad *et al.*, 2019), taste enhancers, and as functional food (da Silva *et al.*, 2016). However, the use of natural products in food and other industrial applications is limited by factors such as the instability of these products to food processing and adverse effects on food sensory and nutritional properties.

Encapsulation of inert bioactive components prevents destructive interaction that might result in the loss of activity (Saikia *et al.*, 2015), regulates release, and ensures masking of unpleasant properties (Rezende *et al.*, 2018). Spray drying and freeze-drying are the most commonly used methods with practical applications in food and pharmaceutical industries.

Alginates are polyanionic copolymers produced by algae species including *Ascophyllum nodosum*, *Laminaria hyperborea*, and *Macrocystis pyrifera*. Alginates are also produced as metabolites by bacteria species such as *Azotobacter* and *Pseudomonas*. However, isolation from bacteria is usually expensive for commercial applications (Goh *et al.*, 2012). The use of alginate in the encapsulation of nutraceuticals and bioactive compounds is widely employed in the food and pharmaceutical sectors (Goh *et al.*, 2012). Sodium carboxymethyl cellulose (CMC) are water soluble, chemically modified natural cellulose with remarkable physical and chemical properties. In the food industry, it is used as stabilizer and thickener, and widely employed in the production of milk drinks, yogurt, ice cream, baked goods, and syrups. Encapsulation of pharmaceuticals and nutraceutical products using blends of sodium alginate and sodium CMC showed good stability with an enhanced release (Lee *et al.*, 2019; Qiu *et al.*, 2020).

Eucalyptus is a plant genus of the family myrtaceae widely used as a source of essential oil. Leaf extract of the specie *E. globulus* is an approved food additive with the Generally Recognized as Safe (GRAS) status. Wood from the specie *E. camaldulensis* is commonly used in the paper industries, and the leaves have been reported to exhibit good antibacterial activity against the foodborne pathogen *Listeria moncytogenes* with good antioxidant properties (Nwabor *et al.*, 2019). In this study, *E. camaldulensis* ethanolic leaf extracts were encapsulated using sodium alginate and sodium CMC as a possible method of preserving the inert bioactive components and incorporation into industrial processing. The microcapsules were characterized tested for micromeritics properties as well as bioactivity and cytotoxicity.

Materials and methods

Materials

Sodium alginate and sodium CMC were purchased from Sigma-Aldrich, Singapore. Tetrazolium bromide (3-(4,5-dimethyl-2-thiazolyl)-2,5-diphenyl-2H, MTT) and trypsin were obtained from Merck (Darmstadt, Germany), Dulbecco's modified eagle medium (DMEM), and foetal bovine serum were purchased from Gibco, UK. All bacteriological media were purchased from Thermo Fisher.

Methods

Extraction procedure

Classified reference voucher specimen of *E. camaldulensis* was deposited at the herbarium of Faculty of Pharmaceutical Sciences, Prince of Songkla University, Thailand. The leaves were extracted by cold maceration method with 95% ethanol as solvent.

Formation of alginate–CMC microcapsules

Alginate–CMC microcapsules were formulated using the freeze-dry method. A 2% sodium alginate solution was mixed with 1% CMC solution in a 1:1 ratio. One millilitre of varying concentrations 250 mg (F1), 500 mg (F2) and 1000 mg (F5) of ethanolic leaf extract of *E. camaldulensis* was then added to the alginate–CMC mixture and allowed to stir for 20 min. The mixture was added dropwise into a 3% $CaCl{\cdot}2H_2O$ solution at a flow rate of 1 ml/10 min under high-speed homogenization at 15 000 rpm. The mixture was left to further homogenize for 60 min and centrifuged at 10 000 rpm for 30 min. Pelleted microcapsules were then freeze dried and pulverized into powder.

Encapsulation yield

The amount of microcapsule (in g) obtained after freeze-drying was calculated as percentage encapsulation yield using the following equation:

$$\%\ \text{Encapsulation yield} = \frac{W_1}{W_2} \times 100$$

where W_1 is the total mass of microcapsules after being freeze dried and W_2 is the mass of Na alginate, CMC, and *E. camaldulensis* extract that were fed in the encapsulation process.

Encapsulation efficiency

Encapsulation efficiency representing the amount of bioactive (extract) encapsulated in the polymer matrix was estimated calorimetrically using the indirect method.

The percentage of encapsulation was calculated using the following equation:

$$\frac{A_{\text{initial}} - A_{\text{supernatant}}}{A_{\text{initial}}} \times 100$$

where A_{initial} is the optical density (OD) of the microcapsule mixture before centrifugation and $A_{\text{supernatant}}$ is the OD of the supernatant after centrifugation.

Particle size analyser

The particle size of the microcapsules was determined using a laser scattering particle size distribution analyser (Horiba LA-300, Japan). The measurements were made in triplicate.

Fourier-transform infrared spectroscopy

Fourier-transform infrared spectroscopy (FTIR) spectra were obtained with a Spectrum 100 series FTIR spectrometer (PerkinElmer) at range 4000 and 650 cm^{-1}.

Micromeritic properties of microcapsules

The micromeritic properties including angle of repose, bulk density, tapped density, Carr's index, and Hausner's ratio were evaluated. The angle of repose was determined by the fixed funnel method using the following equation:

$$\tan\ \theta = \frac{h}{r}$$

where h is height of the microcapsules pile and r is radius of the microcapsules pile.

For determination of bulk and tapped density, microcapsules were tapped using USP tapped density tester (Electrolab, model ETD–1020) for 250 taps and the change in volume was measured. Carr's index and Hausner's ratio were calculated using the following equation:

$$\text{Compressibility index} = \frac{(V_f - V_o) \times 100}{V_o}$$

$$\text{Hausner ratio} = \frac{V_f}{V_o}$$

where *Vo* is the initial volume and *Vf* is the tapped volume.

Determination of moisture (loss on drying)

Loss on drying (LOD) was determined by drying 1 g of microcapsules in an oven at 100–105°C for 3 h and then sample was kept in a desiccator for 24 h and reweighed. The difference in weights was recorded and LOD was calculated using the following equation:

$$\%\ \text{LOD} = \frac{W2 - W3}{W2 - W1} \times 100$$

where W1 is weight of empty weighing bottle, W2 weight of weighing bottle with sample, and W3 is weight of weighing bottle with dried sample.

Determination of swelling index

The swelling index was determined as described by Surini *et al.* (2018) with modifications. Microcapsules (500 mg) were introduced into 10 ml of distilled water and left to stand at 37°C with constant shaking. After 60 min, the microcapsules were centrifuged at 4500 rpm for 10 min and the supernatant was carefully discarded. The swelling index was calculated using the following equation:

$$\text{Swelling index} = \frac{W1 - W2}{W1}$$

where *W1* is weight of microcapsules swelling and *W2* is weight of microcapsules after swelling.

Solubility

The solubility of the formulated micro-capsules was measured as described by Hussain *et al.* (2018), with modifications. Samples weighing 1.0 g were dispersed in 10 ml of distilled water and stirred for 30 min. The mixture was then centrifuged at 3000×*g* for 10 min. The supernatant was oven dried at 105°C for 4 h. The solubility was measured as a result of weight difference and demonstrated in the term of percentage.

Colour measurements

Colour of the microcapsules was determined using a colorimeter (ColorFlex, Hunter Lab Reston, VA, USA), and recorded in terms of L^*, a^*, b^*, where L^* indicates the lightness, a^* redness and greenness, and b^* yellowness and blueness. The manufacturer's standard white plate was used for the calibration (L^* = 92.84; a^* = –1.29; b^* = 0.55). The parameters L^*, a^*, and b^* were used to calculate Chroma, Hue angle, ΔE (total colour change), and browning index

(BI) according to the equations stated by Yeşilsu and Özyurt (2019) and Rigon and Noreña (2016).

$$\text{Chroma} = \sqrt{a*^2 + b*^2}$$

$$\text{Hue} = \tan^{-1}\left(\frac{b^*}{a^*}\right)$$

$$\Delta E = \sqrt{\Delta L^{*2} + \Delta a^{*2} + \Delta b^{*2}}$$

$$\text{BI} = \frac{100(x0.31)}{0.17}$$

where

$$X = \frac{\text{a}^* + 1.75L^*}{5.645L^* + \text{a}^* - 3.012\text{b}^*}$$

Scanning electron microscopy

The morphology of the microcapsules was studied using scanning electron microscopy.

Determination of total phenolic and flavonoid contents of microcapsules

Microcapsules were digested in sodium citrate solution (Pasukamonset *et al.*, 2016). Briefly, 0.1 ml of sample was added to 0.4 ml of Folin-Ciocalteau, and 0.4 ml of Na_2CO_3. The mixture was incubated for 30 min, and the absorbance was read at 700 nm and reported in garlic acid equivalent per milligram sample.

The total flavonoid content was measured using $AlCl_3$. Briefly, 0.1 ml of sample were added to 0.4 ml of distilled water and 30 µl of 5% $NaNO_2$. The mixture was incubated in the dark for 5 min, and 30 µl of a 10% $AlCl_3$ solution was added and incubated for 5 min, and 0.2 ml of a 4% NaOH solution was added. The mixture was incubated in dark for 15 min, and the absorbance was measured at 510 nm and recorded in milligrams of quercetin equivalents (QE) per milligram of the extract.

Antioxidant activities of microcapsules

The antioxidant activity of microcapsules was evaluated using 2,2-diphenyl-1-picrylhydrazyl (DPPH) and 2,2′-azino-bis (3-ethylbenzothiazoline-6-sulfonic acid) (ABTS) radical scavenging assays. The radical scavenging activity was calculated using the following equation:

$$\%\ \text{Inhibition} = \frac{A_{\text{cont}} - A_{\text{test}}}{A_{\text{cont}}} \times 100$$

where A_{cont} is the absorbance of the negative control and A_{test} is the difference of the absorbance of samples and corresponding blank.

In vitro release of polyphenols from microparticles

Release of polyphenols was estimated by quantifying the phenolic content released from the microcapsules using Folin–Ciocalteau method (Arriola *et al.*, 2016). Briefly, 200 mg of the microcapsules was suspended in 5 ml of distilled water at 4 and 37°C with constant stirring at 150 rpm. At interval, an aliquot of the supernatant was withdrawn with replacements and the phenolic content was quantified. Obtained results were expressed in milligrams of garlic acid equivalent GAE per milligram of dry microparticles. Experiments were recorded in triplicate. Released polyphenol content was calculated using the equation:

$$\text{Polyphenols released}\ (\%) = \frac{TP_t}{TP_\infty} \times 100$$

where TP_t is the phenolic content released at time t and TP_∞ is the total phenolic content of the microcapsules.

Values were fitted into various kinetic models, equation, and coefficient of correlation (r) values were calculated for linear curves by regression analysis of the plots.

Antimicrobial activities of microcapsules

The antimicrobial activities of microcapsules were determined using the standard broth micro-dilution method (CLSI, 2015). Minimum inhibitory concentrations and minimum bactericidal concentrations were recorded after 24 h incubation at 37°C. All experiments were set up in triplicate.

Cell culture and cytotoxicity

Human embryonic colon cells Caco-2 were cultured in high glucose DMEM supplemented with 10 per cent foetal bovine serum and 1 per cent antibiotics. The cells were incubated at 37°C with 5% CO_2. Cells 1×10^4 cells/well were seeded in 96-well microtitre plates and incubated overnight.

Toxicity of the microcapsules was evaluated on Caco-2 cells using MTT assay at 570 nm. Cell viability was calculated as

$$\%\ \text{Cell viability} = \frac{\text{OD treatment}}{\text{OD control}} \times 100$$

Statistical analysis

All experiment was performed in triplicate and the mean values were recorded. Results were analysed using the analysis of variance (ANOVA). SPSS 20 was used for the analysis and a 95% confidence interval was maintained throughout the experiment (Scheffe test at $P < 0.05$).

Results and Discussion

Particle size

The particle size of microcapsules was reported based on the equivalent sphere concept (Table 1). The D_{50} values of the microcapsules ranged from 6.7 to 26.6 µm, with the F0 presenting the lowest particle size of 6.7 µm. Addition of extract resulted in a significant ($P < 0.05$) increase in the diameter of the microcapsules; however, particle size diameter was not extracted concentration dependent. Factors including concentration of crosslinking agent,

Table 1. Particle size of freeze-dried microcapsules

Formulations	Particle size (µm)			
	D_{10}	D_{50}	D_{90}	Span
F0	3.07	6.70	14.63	1.73
F1	11.85	26.59	59.70	1.79
F2	4.99	10.03	20.15	1.51
F5	4.41	9.06	18.61	1.56

D_{10}, 10th percentile of cumulated volume distribution; D_{50}, median particle diameter (50th percentile) of cumulated volume distribution; D_{90}, 90th percentile of cumulated volume distribution.

homogenization speed, and time might affect the size of the microcapsules. Low span values were observed for the microcapsules, indicating a narrow particle size distribution.

Percentage yield and encapsulation efficiency

Percentage yield and encapsulation efficiency are important factors for a microencapsulation process. Percentage yield measures material recovery during an encapsulation process and signifies process suitability. In this study, a high percentage yield (70.4%–81.5%) was observed, demonstrating a minimal loss of material (Table 2). Various factors including concentration of polymers, solubility, concentration of the crosslinking agent, and viscosity of the mixture might affect the yield. Similarly, encapsulation efficiency is a measure of the percentage of the core active agent loaded in the microcapsules (Choi and Chang, 2018). In addition, it reflects the degree of protection provided by the encapsulant (Binsi *et al.*, 2017). Encapsulation of the extract using alginate–CMC demonstrated %EE of 74.2 ± 0.011%–82.43 ± 0.772% (Table 2). The high encapsulation efficiency shows the compatibility of alginate with CMC and further suggests the formation of stable interactions between reactive sites of the polymers and the extract.

Physicochemical properties of microcapsules

Physicochemical parameters of the microcapsules including zeta potentials, polydispersity index, swelling index, and solubility are presented in (Table 2). Zeta potential is an important parameters that indicates charge and stability against coalescence and aggregation (Sezgin-Bayindir *et al.*, 2015). The alginate–CMC encapsulated extract showed a zeta potential of –11.01, –17.01, 2.23, and –2.45 for F0, F1, F2, and F5, respectively. As zeta potential decreases, the particles attract one another forming aggregates. Zeta potentials ≥ ±30 mV are generally regarded as stable (Wang *et al.*, 2016); hence, the formulations showed low electrostatic stabilization with net charges closer to zero. It has been reported previously that the ratio of polymers is an important surface charge modulating factors (Caetano *et al.*, 2016).

Polydispersity index (PDI) of a polymer colloidal system indicates the uniformity of the colloidal particles in the solution (distribution of size populations within a sample). In this study, PDI values of the microcapsules ranged from 0.344 to 0.489, indicating a high size dispersion (Danaei *et al.*, 2018). The result confirms the high range between the D_{10} and D_{90} values of the microcapsules.

The microcapsules exhibited a high swelling index that reduced with increased extract concentration. The high swelling index of the alginate–CMC co-polymer microcapsules reflects the hydrophilic nature of alginate and hydrocolloidal properties of CMC. Alginate has been reported to exhibit high swelling properties at neutral and alkaline pH (Akalin and Pulat, 2018), whereas Na-CMC demonstrates a pH-independent swelling property (El-Hag Ali *et al.*, 2008). Results revealed that addition of the extract significantly ($P < 0.05$) reduced the swelling index. Increase in extract concentration further lowered the swelling index of the microcapsules. This might be as a result of pH alterations and the formation of intra-molecular hydrogen bonds. For effective release of core material, the microcapsules must absorb solvent and swell significantly (Patel *et al.*, 2016), thus the results suggested that alginate–CMC co-polymer blend might be an effective release wall material for the encapsulation of bioactive compound.

The microcapsules demonstrated a poor solubility in water that ranged between approximately 19 and 22%. Addition of the extract showed a slight concentration-dependent reduction in solubility. Reduction in solubility might be as a result of alterations in pH resulting in the insolubility of alginate and sodium CMC or the formation of complex electrostatic bonding between the polymers and the extract.

Micromeritic properties of microcapsules

The micromeritics properties of microcapsules are presented in Table 3. The results indicated that microcapsules showed poor flow property as shown be Carr's index between 27 and 40, angle of repose between 27.9° and 30.9°, and Hausner's ratio >1.5, indicating a passable flow behaviour of the microcapsules. The results further revealed that the F1 had the highest tapped density, which might be due to the relatively larger particle size as revealed by the D_{50} suggesting a reduction in the cohesive force between particles. In addition, moisture content of the microcapsules might also affect its flowability as a result of liquid bridge forces due to the presence of thin-film liquids on the surface of the microparticles. Formulation F1 displayed the least moisture content while F5 showed the highest percentage of moisture loss. The swelling index of the microcapsules varied inversely with the concentration of the loaded extract. F0 showed the highest swelling index, while F5 showed the least. The reduction in swelling index observed in the extract loaded microcapsules is attributed to the decrease in water-holding capacity resulting from the increase in concentration of extract.

Table 2. Physicochemical properties of microcapsules

Formulations	% Yield	Encapsulation efficiency (%)	Swelling index (%)	Polydispersity index	Zeta potential (mV)	Solubility (%)
F0	80.7	NA	84.0	0.450	–11.01	22.2 ± 1.1
F1	76.5	74.2 ± 0.01	81.4	0.489	–17.01	22.1 ± 1.6
F2	81.5	80.11 ± 0.01	71.8	0.344	2.23	19.9 ± 0.1
F5	70.4	82.43 ± 0.77	54.4	0.370	–2.45	18.8 ± 0.2

NA, not applicable.

Table 3. Micromeritics properties of microcapsules

Samples	Bulk density (g/cc)	Tapped density (g/cc)	Moisture loss (%)	Angle of repose (°)	Carr's index	Hausner's ratio
Blank	0.22 ± 0.02	0.38 ± 0.04	14.7 ± 0.02	30.9 ± 1.41	40	1.66
F1	0.24 ± 0.03	0.44 ± 0.01	9.0 ± 0.03	29.24 ± 1.15	44	1.8
F2	0.27 ± 0.01	0.41 ± 0.06	14.0 ± 0.01	29.68 ± 0.83	34	1.5
F5	0.24 ± 0.07	0.33 ± 0.03	15.0 ± 0.04	27.9 ± 3.22	27	1.38

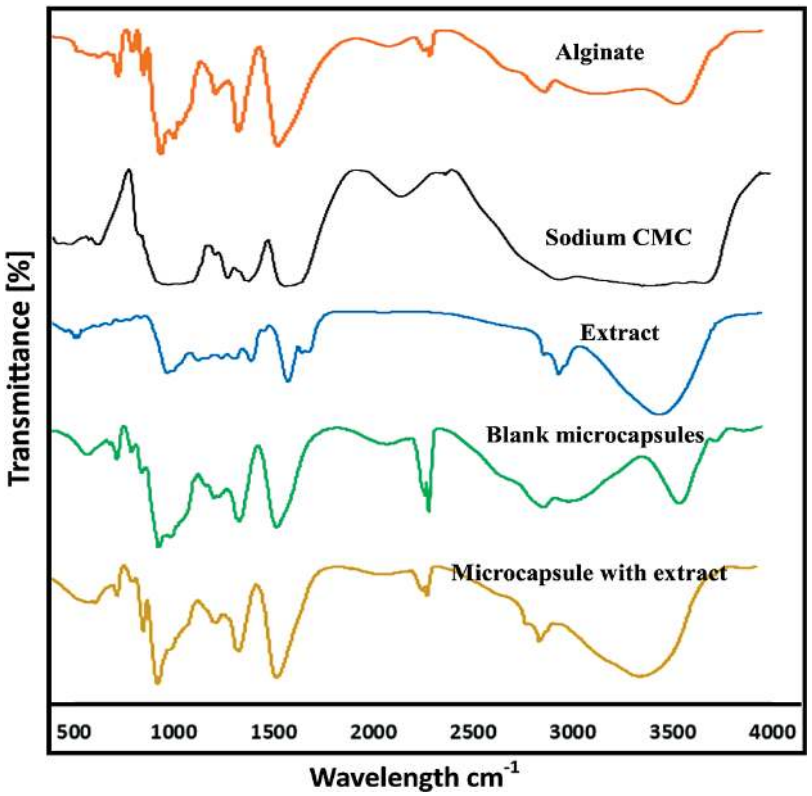

Figure 1. FTIR spectra of polymers, extract and microcapsules recorded between 500 and 3900 nm, showing molecular interaction of components following the encapsulation process.

Fourier-transformed infrared spectroscopy

The Fourier-transformed infrared spectroscopy (FTIR) spectra of the polymers, extract, and microcapsules is shown in Figure 1. The spectra showed molecular interactions between functional groups resulting in the formation of new groups and/or alteration of already existing groups. Similar bands were observed for all the spectra with broad bands at 3400–3600 cm^{-1} attributed to the O–H vibrations, while the peaks at 2900–2950 cm^{-1} relates to the C–H bands. Peaks between 1600–1650 cm^{-1} and 1420–1450 cm^{-1} represented the asymmetric and symmetric stretching of the –COO– (Capanema *et al.*, 2018). The extract spectra showed a peak at 1726 cm^{-1}, which was ascribed to C=O group. The spectra around 2360 cm^{-1} represents CO_2 stretching that might have resulted from measurement condition. Addition of the extract resulted in minor shifts in bands as shown by the difference between spectra of blank microcapsule, a microcapsule with extract. The prominent C–H peak located at 2928 and 2950 cm^{-1} in the extract and blank capsules combined, resulting in a minor shift to 2926 cm^{-1}.

Total phenolic and flavonoid

Total phenolic content (TPC) and total flavonoid content (TFC) of the microcapsules are presented in Figure 2. The results indicated a TPC of 0.26, 0.15, and 0.09 mg garlic acid equivalent/mg sample for formulation F5, F2, and F1 and a TFC of 0.21, 0.09, and 0.06 mg catechin equivalent/mg sample for F5, F2, and F1, respectively. The phenolic and flavonoid contents of the microcapsules indicate the effective encapsulation of the extract. Polyphenols are excellent bioactive components with good antioxidant and antimicrobial properties that can be explored for food preservation and shelf-life extension.

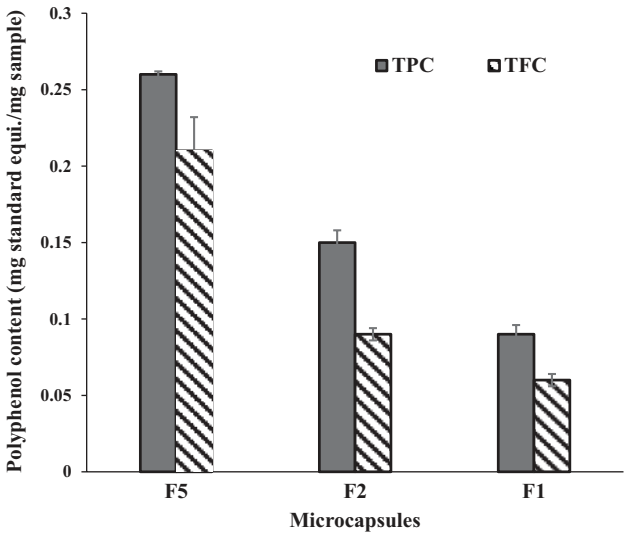

Figure 2. Total phenolic content (TPC) and total flavonoid content (TFC) of the microcapsules tested using Folin–Ciocalteu and $AlCl_3$ assay.

Antioxidant efficacy of microcapsules

The antioxidant activities of the microcapsules, demonstrated by DPPH and ABTS assay, are shown in Figure 3. The capsules showed

a concentration-dependent inhibition for both DPPH and ABTS. The concentration of the extract in the microcapsules was reflected in the antioxidant properties, hence F5 showed the highest antioxidant properties whereas F1 showed the least antioxidant activity. The results of the antioxidant assay indicated that encapsulation using the polymers did not alter the bioactive properties of the extract. It further suggested the excellent release of the polyphenols from the polymers matrix. The antioxidant properties of plant polyphenols in food enhances the shelf-life of products through inhibition of enzymatic oxidative processes such as lipid peroxidation.

Release of polyphenols

The release of polyphenols from the alginate–CMC matrix, evaluated at 37°C and 4°C, is presented in Figure 4. The results indicated a significant difference in the release profile at the tested temperatures ($P < 0.05$). The microcapsules at both temperatures showed a rapid release of polyphenols within 1 h. Encapsulation of *Stevia rebaudiana* leaf extract and *Clitoria ternatea* petal flower extract with alginate showed similar results (Arriola *et al.*, 2016; Pasukamonset *et al.*, 2016). However, the present study indicated a slow and regulated release of polyphenol over a wide time range. In addition, the microcapsules showed higher polyphenol release at 37°C than at the storage temperature of 4°C. This might be as a result of increased collision due to increase in Brownian movement of particles.

Release of polyphenols at 37°C, followed the first-order kinetics with dependence on concentration and a zero-order kinetics independent of concentration at 4°C. The Higuchi kinetic model showed a time-dependent controlled release at 37°C, and a time-independent controlled release at 4°C.

Antimicrobial activity of microcapsules

Antimicrobial activities of the encapsulated extracts of *E. camaldulensis* against foodborne pathogenic bacteria are shown in Table 4. The microencapsulated extracts demonstrated antimicrobial effects with minimum inhibitory concentrations and minimum bactericidal concentrations ranging from 0.19 to 3.12 and 0.19 to 12.25 mg/ml, respectively. In addition, no antimicrobial activity was observed for F0. The results suggested an antimicrobial activity dependant on the concentration of the extract. Furthermore, the antimicrobial activity observed suggests the release of core material

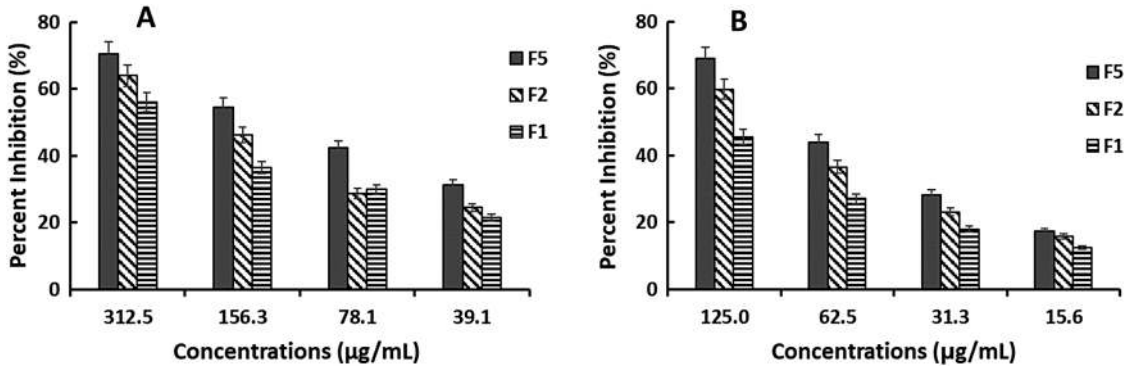

Figure 3. Antioxidant properties of microcapsules evaluated using DPPH (A) and ABTS (B).

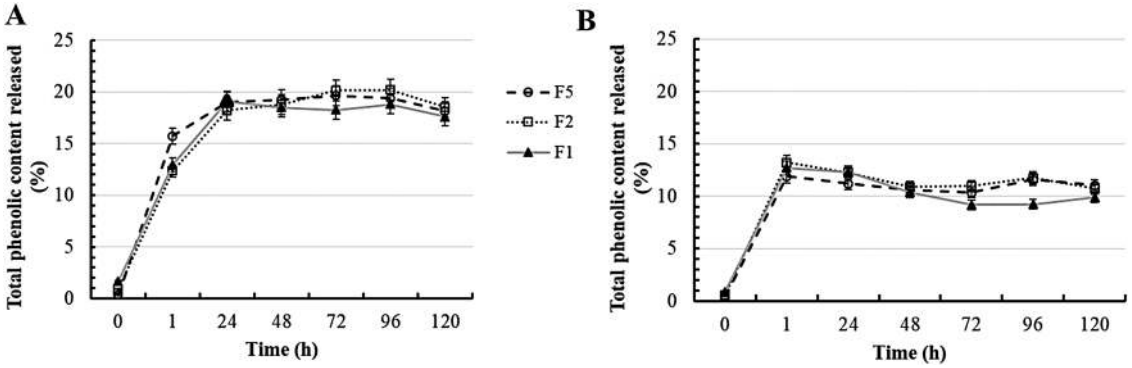

Figure 4. Release profile of polyphenols evaluated at 37°C (A) and 4°C (B).

Table 4. Antimicrobial activities of microcapsules and extract

Isolates	MIC/MBC (mg/ml)				
	Blank	F1	F2	F5	Extract
Bacillus cereus	>24	0.39/1.56	0.19/0.39	0.19/0.19	0.064/0.128
Listeria monocytogenes	>24	1.56/6.25	0.39/6.25	0.19/0.78	0.128/0.512
Staphylococcus aureus	>24	3.12/12.25	1.56/6.25	0.39/1.56	0.128/0.256

Table 5. Colour parameters of microcapsules

	*L**	*a**	*b**	*ΔE*	Chroma	Hue	BI
Blank	9.17 ± 0.13[a]	−0.69 ± 0.13[a]	−1.54 ± 0.15[a]	9.33 ± 0.13[a]	1.72 ± 0.06[a]	1.15 ± 0.20[a]	−20.26 ± 0.98[a]
F1	29.43 ± 0.12[a]	−5.13 ± 0.09[ab]	8.78 ± 0.22[a]	31.14 ± 0.18[ab]	10.17 ± 0.23[a]	−1.04 ± 0.01[ab]	20.38 ± 0.77[a]
F2	28.05 ± 0.10[ab]	−4.83 ± 0.05[ac]	13.26 ± 0.44[a]	31.40 ± 0.18[ac]	14.11 ± 0.41[a]	−1.22 ± 0.01[acd]	46.91 ± 2.79[a]
F5	27.97 ± 0.04[ac]	−3.15 ± 0.08[a]	18.94 ± 0.47[a]	33.93 ± 0.24[a]	19.20 ± 0.46[a]	−1.41 ± 0.01[abe]	93.45 ± 4.14[a]

Values represent mean values ± standard deviation. Same superscript within the same column indicates significant difference while different superscript indicates no significant difference at $P < 0.05$.

Table 6. Pearson correlation coefficients (*r*) between colour parameters (*L**, *a**, *b**, *ΔE*, Chroma, Hue, and BI)

	*L**	*a**	*b**	*ΔE*	Chroma	Hue	BI
*L**	1						
*a**	−0.918**	1					
*b**	0.846**	−0.596**	1				
ΔE	0.987**	−0.849**	0.921**	1			
Chroma	0.833**	−0.575**	1.000**	0.911**	1		
Hue	−0.979**	0.848**	−0.927**	−0.995**	−0.917**	1	
BI	0.735**	−0.432	0.981**	0.835**	0.986**	−0.841**	1

*Correlation is significant at the 0.01 level (two-tailed).

across the walls of the particles into the media. Microbial contamination of food products is a leading cause of food spoilage and foodborne disease outbreaks, thus inhibiting the growth of microorganism in food is fundamental to food preservation and shelf-life extension. The results of this study revealed that the encapsulated plant polyphenols demonstrated antimicrobial activities and could be used as an antimicrobial preservative agent.

Colour analysis

The result of colour analysis revealed lightness (*L**), Chroma and Hue angle of the microcapsules (Table 5). The redness and yellowness values *a** and *b** of the blank microcapsules were −0.69 ± 0.13 and −1.54 ± 0.15. The redness/blueness values increased in F1 but reduced with the addition of more extract in F2 and F5. Yellowness/greenness values displayed a significant ($P < 0.05$) extract concentration-dependent increase. A negative correlation was observed between redness *a**, greenness *b** values, and the lightness values *L**. Chroma was positively correlated with *L**, whereas Hue displayed a negative correlation (Table 6). The brownness index BI of the microcapsules increased with increase in the extract concentration added. The results demonstrated that the polymers used were not effective at masking the colour of the extract, hence addition of the microcapsules into food products might impair the colour appeal of the product resulting in reduced consumers demand or rejection of the product.

Scanning electron microscopy

The micrograph showed irregular shape and compact structure similar to previously observed micrographs for freeze-dried microcapsules (Kuck and Noreña, 2016; Hussain *et al.*, 2018; Yang *et al.*, 2019) Figure 5. The high-speed homogenization and breakage of microbeads formed after cross-linking into irregular shapes, and the crushing procedure employed for size reduction after lyophilization might be responsible for the irregular-shaped observed. In addition, no difference in structure was observed from the scanning electron micrograph of the different formulations. However, the micrograph showed a larger particle size for F0 and F1 which might be due to clumping and aggregation of particles.

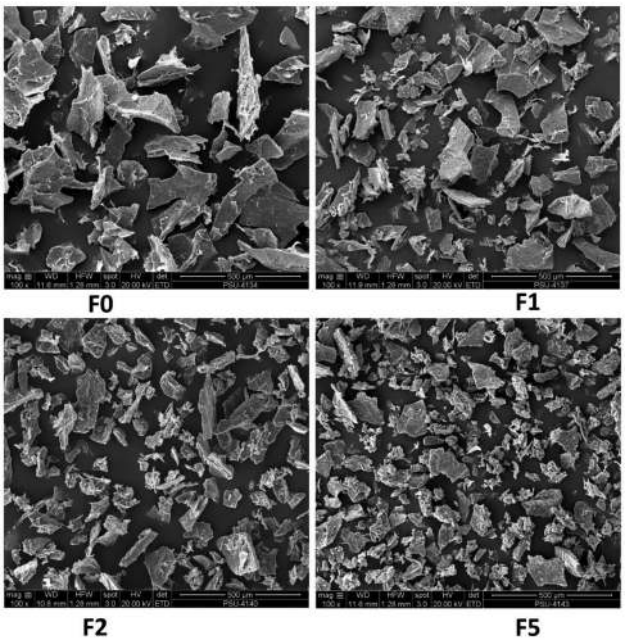

Figure 5. Scanning electron micrograph of microcapsules, showing the shape and surface morphology of the microcapsules.

Cytocompatibility testing of microcapsules

The cytotoxicity evaluation of eluates obtained from microcapsules at various time intervals against human embryonic colon cell Caco-2 is shown in Figure 6. At the tested time intervals, eluates from the formulations showed >80% cell viability when compared with the control (100%). The cytocompatibility of microencapsulated plant extracts and phytochemicals have been reported for various mammalian cell lines (Condurache *et al.*, 2019; Mohammed *et al.*, 2019;

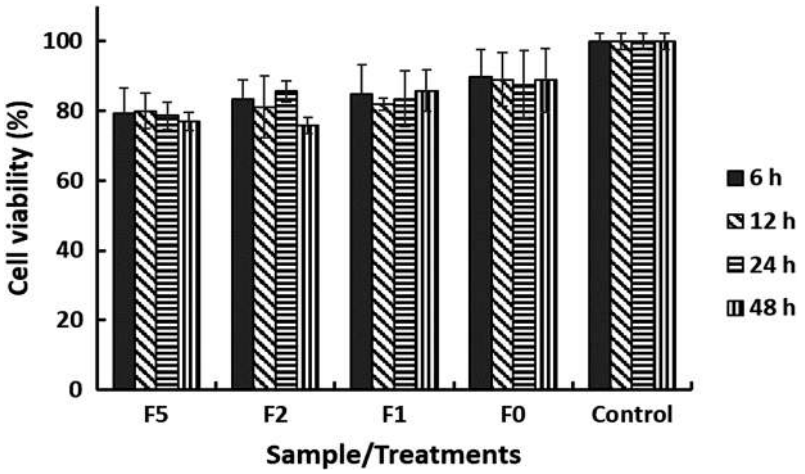

Figure 6. Cytotoxicity of eluates from microcapsules at various hours, on human embryonic colon cell Caco-2.

Ruiz-Montañez *et al.*, 2019). Encapsulation of active compounds can reduce the adverse effects through regulated slow release with prolonged activity.

Conclusions

Microencapsulation of bioactive compounds using bio-friendly non-toxic polymers is employed in food, pharmaceutical, and cosmetic industries for the incorporation of active compounds into products. Microencapsulation preserves the activity of liable bioactive compounds and masks unpleasant properties of the bioactive. Encapsulation of ethanolic extracts of *E. camaldulensis* using sodium alginate and sodium CMC as wall material yielded stable microcapsules with antimicrobial and antioxidant properties. The microcapsules demonstrated good physical, structural, and micromeretics properties. In addition, the capsules showed delayed and regulated release and were cytocompatibility with human colon cells. The results suggested that encapsulation using alginate and sodium CMC can be employed for the incorporation of plant bioactive compounds into products.

Funding

This work was supported by Thailand's Education Hub for ASEAN Countries (Grant No. TEH-AC 013/2017) and the TRF Senior Research Scholar (Grant no. RTA 6180006), The Thailand Research Fund.

Conflict of interest

The authors declare no conflict of interest.

References

Akalin, G. O., Pulat, M. (2018). Preparation and characterization of nanoporous sodium carboxymethyl cellulose hydrogel beads. *Journal of Nanomaterials*, 2018: 1–12.

Allahdad, Z., Varidi, M., Zadmard, R., *et al.* (2019). Binding of β-carotene to whey proteins: multi-spectroscopic techniques and docking studies. *Food Chemistry,* 277: 96–106.

Arriola, N. D. A., De Medeiros, P. M., Prudencio, E. S., *et al.* (2016). Encapsulation of aqueous leaf extract of *Stevia rebaudiana* bertoni with sodium alginate and its impact on phenolic content. *Food Bioscience*, 13: 32–40.

Binsi, P., Nayak, N., Sarkar, P., *et al.* (2017). Structural and oxidative stabilization of spray dried fish oil microencapsulates with gum arabic and sage polyphenols: characterization and release kinetics. *Food Chemistry,* 219: 158–168.

Caetano, L., Almeida, A., Gonçalves, L. (2016). Effect of experimental parameters on alginate/chitosan microparticles for bcg encapsulation. *Marine Drugs*, 14(5): 90.

Capanema, N. S., Mansur, A. A., de Jesus, A. C., *et al.* (2018). Superabsorbent crosslinked carboxymethyl cellulose-PEG hydrogels for potential wound dressing applications. *International Journal of Biological Macromolecules*, 106: 1218–1234.

Choi, Y. R., Chang, Y. H. (2018). Microencapsulation of gallic acid through the complex of whey protein concentrate-pectic polysaccharide extracted from *Ulmus davidiana*. *Food Hydrocolloids*, 85: 222–228.

CLSI. (2015). Methods for antimicrobial dilution and disk susceptibility testing of infrequently isolated or fastidious bacteria. *Proposed Guideline*, 35: 64–69.

Condurache, N. N., Aprodu, I., Crăciunescu, O., *et al.* (2019). Probing the functionality of bioactives from eggplant peel extracts through extraction and microencapsulation in different polymers and whey protein hydrolysates. *Food and Bioprocess Technology*, 12: 1316–1329.

Danaei, M., Dehghankhold, M., Ataei, S., *et al.* (2018). Impact of particle size and polydispersity index on the clinical applications of lipidic nanocarrier systems. *Pharmaceutics*, 10(2): 57.

Da Silva, B. V., Barreira, J. C., Oliveira, M. B. P. (2016). Natural phytochemicals and probiotics as bioactive ingredients for functional foods: extraction, biochemistry and protected-delivery technologies. *Trends in Food Science and Technology*, 50: 144–158.

Dhiman, R., Aggarwal, N. K. (2019). Efficacy of plant antimicrobials as preservative in food. In: Socaci, S. A., Frca A. C., Aussenac T. and Laguerre J.-C., eds. *Food Preservation and Waste Exploitation*, IntechOpen.

Dikshit, R., Tallapragada, P. (2018). Comparative study of natural and artificial flavoring agents and dyes. In: Grumezescu A. M., Holban A. M., eds., *Handbook of Food Bioengineering, Natural and Artificial Flavoring Agents and Food Dyes*, Academic Press, 83–111.

El-hag, A. A., Abd El-rehim, H. A., Kamal, H., *et al.* (2008). Synthesis of carboxymethyl cellulose based drug carrier hydrogel using ionizing radiation for possible use as site specific delivery system. *Journal of Macromolecular Science®, Part A: Pure and Applied Chemistry*, 45(8): 628–634.

Goh, C. H., Heng, P. W. S., Chan, L. W. (2012). Alginates as a useful natural polymer for microencapsulation and therapeutic applications. *Carbohydrate Polymers*, 88(1): 1–12.

Hussain, S., Hameed, A., Nazir, Y., *et al.* (2018). Microencapsulation and the characterization of polyherbal formulation (phf) rich in natural polyphenolic compounds. *Nutrients*, 10(7): 843.

Kuck, L. S., Noreña, C. P. (2016). Microencapsulation of grape (*Vitis labrusca* var. Bordo) skin phenolic extract using gum Arabic, polydextrose, and partially hydrolyzed guar gum as encapsulating agents. *Food Chemistry,* 194: 569–576.

Lee, C. H., Nalluri, L. P., Popuri, S. R. (2019). Optimization studies for encapsulation and controlled release of curcumin drug using Zn^{+2} cross-linked alginate and carboxy methylcellulose blend. *Journal of Polymer Research*, 26(1): 13.

Mohammed, H. A., Al-Omar, M. S., El-Readi, M. Z., *et al.* (2019). Formulation of ethyl cellulose microparticles incorporated pheophytin a isolated from suaeda vermiculata for antioxidant and cytotoxic activities. *Molecules*, 24(8): 1501.

Nwabor, O. F., Vongkamjan, K., Voravuthikunchai, S. P. (2019). Antioxidant properties and antibacterial effects of eucalyptus camaldulensis ethanolic leaf extract on biofilm formation, motility, hemolysin production, and cell membrane of the foodborne pathogen *Listeria monocytogenes*. *Foodborne Pathogens and Disease,* 16(8): 581–589.

Pasukamonset, P., Kwon, O., Adisakwattana, S. (2016). Alginate-based encapsulation of polyphenols from clitoria ternatea petal flower extract enhances stability and biological activity under simulated gastrointestinal conditions. *Food Hydrocolloids*, 61: 772–779.

Patel, N., Lalwani, D., Gollmer, S., *et al.* (2016). Development and evaluation of a calcium alginate based oral ceftriaxone sodium formulation. *Progress in Biomaterials,* 5(2): 117–133.

Qiu, B., Tian, H., Yin, X., *et al.* (2020). Microencapsulation of 2-phenyl ethanol with methylcellulose/alginate/methylcellulose as the wall material and stability of the microcapsules. *Polymer Bulletin*, 77(2): 989–1001.

Rezende, Y. R. R. S., Nogueira, J. P., Narain, N. (2018). Microencapsulation of extracts of bioactive compounds obtained from acerola (*Malpighia emarginata* DC) pulp and residue by spray and freeze drying: chemical, morphological and chemometric characterization. *Food Chemistry,* 254: 281–291.

Rigon, R. T., Zapata Noreña, C. P. (2016). Microencapsulation by spray-drying of bioactive compounds extracted from blackberry (*Rubus fruticosus*). *Journal of Food Science and Technology,* 53(3): 1515–1524.

Ruiz-Montañez, G., Calderón-Santoyo, M., Chevalier-Lucia, D., *et al.* (2019). Ultrasound-assisted microencapsulation of jackfruit extract in eco-friendly powder particles: characterization and antiproliferative activity. *Journal of Dispersion Science and Technology*, 40(10):1507–1515.

Saikia, S., Mahnot, N. K., Mahanta, C. L. (2015). Optimisation of phenolic extraction from *Averrhoa carambola* pomace by response surface methodology and its microencapsulation by spray and freeze drying. *Food Chemistry,* 171: 144–152.

Sezgin-Bayindir, Z., Antep, M. N., Yuksel, N. (2015). Development and characterization of mixed niosomes for oral delivery using *Candesartan cilexetil* as a model poorly water-soluble drug. *AAPS Pharmscitech,* 16(1): 108–117.

Surini, S., Nursatyani, K., Ramadon, D. (2018). Gel formulation containing microcapsules of grape seed oil (*Vitis vinifera* L.) for skin moisturizer. *Journal of Young Pharmacists*, 10(1): 41.

Wang, L., Gao, Y., Li, J., *et al.* (2016). Effect of resveratrol or ascorbic acid on the stability of α-tocopherol in O/W emulsions stabilized by whey protein isolate: simultaneous encapsulation of the vitamin and the protective antioxidant. *Food Chemistry,* 196: 466–474.

Yang, W., Wang, L., Ban, Z., *et al.* (2019). Efficient microencapsulation of syringa essential oil; the valuable potential on quality maintenance and storage behavior of peach. *Food Hydrocolloids*, 95: 177–185.

Yeşilsu, A. F., Özyurt, G. (2019). Oxidative stability of microencapsulated fish oil with rosemary, thyme and laurel extracts: a kinetic assessment. *Journal of Food Engineering*, 240: 171–182.